Research Article

Received: 6 April 2020 Revised: 9 December 2020 Accepted article published: 12 December 2020 Published online in Wiley Online Library:

(wileyonlinelibrary.com) DOI 10.1002/ps.6234

Effects of non-thermal plasma technology on *Diaporthe longicolla* cultures and mechanisms involved

María C Pérez-Pizá,[a] Pablo E Grijalba,[b] Ezequiel Cejas,[c] Juan C Chamorro Garcés,[c] Matías Ferreyra,[c] Carla Zilli,[a] Pablo Vallecorsa,[a] Diego Santa-Cruz,[d] Gustavo Yannarelli,[d] Leandro Prevosto[c†] and Karina Balestrasse[a†*]

Abstract

BACKGROUND: The *Diaporthe/Phomopsis* complex (D/P) is a group of soybean seed-borne fungi. The use of chemical fungicides, either for seed treatment or during the crop cycle, is the most adopted practice for treating fungal diseases caused by this complex. Worldwide, there is a search for alternative seed treatments that are less harmful to the environment than chemicals. Non-thermal plasma (NTP) is a novel seed treatment technology for pathogen removal. This research aimed to evaluate the effects of NTP on the *in vitro* performance of pure cultures of *Diaporthe longicolla* and elucidate the mechanisms underlying these effects.

RESULTS: Active *D. longicolla* mycelium, growing *in vitro*, was exposed to different NTP treatments, employing a dielectric barrier discharge arrangement with different carrier gases (N_2 or O_2). Fungal growth, fresh biomass and colony appearance were negatively affected by plasma treatments (TN3 and TO3). Lipid peroxidation and antioxidant activities were higher in plasma-treated colonies comparison with non-exposed colonies (control). Fungal asexual spores (conidia) were also exposed to NTP, showing high susceptibility.

CONCLUSION: Exposure of *D. longicolla* colonies to NTP severely compromised fungal biology. Ozone production during treatment and lipid peroxidation of fungal cell membranes appeared to be involved in the observed effects.

Supporting information may be found in the online version of this article.

Keywords: *Diaporthe longicolla*; soybean seed decay; non-thermal plasmas; fungal growth

1 INTRODUCTION

The *Diaporthe/Phomopsis* complex (D/P) is a group of phytopathogenic fungi that may affect soybean crop, causing significant economic losses,[1, 2] mostly associated with seed deterioration.[3] These fungi are known to be seed-borne as they may colonize the internal tissues of seeds.[4, 5] In the field, initial infections may proceed either from sowing infected seeds or from spores in stubble that reach the plant via rain splashes.[6] Whenever rainy conditions delay normal harvest, the diseases caused by this complex may reduce seed weight by 10% and germination by 50%.[7] Among the management strategies used for this type of disease, Ploper and Backman[8] cite use of high-quality seed or application of chemical fungicides either as a seed treatment before sowing or during the crop cycle. Chemical fungicides are considered the most reliable and efficient treatment for managing fungal pathogens.[9, 10] In the context of climate change, the prevailing need to rationalize and reduce the use of agrochemicals is currently one of the most urgent issues demanding the attention of researchers, and cleaner management strategies are being sought around the world.

* *Correspondence to: K Balestrasse, Facultad de Agronomía, Universidad de Buenos Aires, San Martín 4453, 1417 Buenos Aires, Argentina. E-mail: kbale@agro.uba.ar*

† *Leandro Prevosto and Karina Balestrasse are joint research directors.*

a *Instituto de Investigaciones en Biociencias Agrícolas y Ambientales (INBA), Facultad de Agronomía, Universidad de Buenos Aires (UBA), Consejo Nacional de Investigaciones Científicas y Técnicas (CONICET), Buenos Aires, Argentina*

b *Cátedra de Fitopatología, Departamento de Producción Vegetal, Facultad de Agronomía, Universidad de Buenos Aires, Facultad de Agronomía, Buenos Aires, Argentina*

c *Departamento de Ingeniería Electromecánica, Grupo de Descargas Eléctricas, Facultad Regional Venado Tuerto, Universidad Tecnológica Nacional, CONICET, Venado Tuerto, Argentina*

d *Laboratorio de Regulación Génica y Células Madre, Instituto de Medicina Traslacional, Trasplante y Bioingeniería (IMeTTyB), Universidad Favaloro-CONICET, Buenos Aires, Argentina*

Non-thermal plasma (NTP) is a novel technology considered suitable for treating biological targets with the aim of sterilization. Its active agents [reactive oxygen species (ROS), reactive nitrogen species (RNS), ultraviolet (UV) radiation and charged particles, including energy electrons] are capable of removing microorganisms and degrading mycotoxins (and other compounds) from biological surfaces, without damaging the exposed targets or the environment because no residues remain after its use.[11, 11,12] Several reports in the past decade have demonstrated the effectiveness of NTP for the inactivation or removal of a wide range of different microorganisms.[11, 13–15] Nevertheless, the mechanisms of inactivation are still being intensively explored and discussed.[16, 17] Although each reactive substance can affect cells independently, it has been suggested that inactivation of microorganisms results from their synergistic effects.[18] Thereby, NTP may exhibit different modes of action: cell surface erosion,[19, 20] lipid peroxidation,[20–22] enzyme activity alteration,[20, 23] protein denaturation,[19, 24] and DNA degradation.[23]

To date, research concerning fungal removal using plasma technology has mostly studied certain types of fungi: clinical,[25, 26] food-borne,[27, 28] and seed/fruit contaminants.[20, 29] According to Misra *et al.*,[30] external contamination of seeds and fruits can be easily resolved through plasma treatment, but the limits to how far plasma active agents may penetrate tissues are unclear and deserve further study. In recent investigations,[31, 32] we generated plasma through dielectric barrier discharges (DBD) and demonstrated that it can remove D/P fungi from soybean seeds, highlighting the ability of active species to penetrate the internal tissues of seeds and eliminate fungal mycelium. The current research aimed to demonstrate the effects of NTP on pure cultures of *D. longicolla* and to elucidate the mechanisms underlying the plasma removal effect when applied to seeds. To achieve this, active mycelium was exposed to different *in vitro* treatments, employing a DBD arrangement with one layer of a polyester film (dielectric barrier), different carrier gases (N_2 or O_2) and an exposure time of 3 min. After plasma treatments, exposed colonies were analyzed for fungal growth and structural changes compared with non-exposed colonies (control). Afterward, mycelia were analyzed to detect biochemical changes. Fungal asexual spores (conidia) were also exposed to determine their susceptibility to plasma treatments.

2 MATERIALS AND METHODS

2.1 Fungal material

2.1.1 Morphological characterization

D/P isolates were obtained from symptomatic soybean seeds (variety DM 53i53 IPRO). Seeds were superficially disinfected (1% sodium hypochlorite for 60 s), sown in Petri dishes containing 25 cm^3 of sterilized potato dextrose agar (PDA) and incubated under controlled conditions (25 ± 2 °C, in darkness) for 7 days. Afterward, dishes were analyzed for D/P detection, according to ISTA Rules.[33] Those fungi that, according to Scandiani and Luque,[34] exhibited a D/P-like morphology were isolated in PDA (Figure S1) and incubated in a growth chamber (25 °C and 12:12 h light/dark photoperiod) for 10 days. To visualize sexual and asexual structures, isolates were transferred to PDA containing sterile soybean stems and incubated at 25 °C and a 12:12 h light/dark photoperiod for 40 days.[34, 35] Isolates were morphologically characterized considering color, type of mycelium, presence and type of stroma, presence of pycnidia, presence and type of conidia, and presence and type of sexual structures.[34, 36]

2.1.2 Fungi molecular identification by PCR of ITS region

Monosporic cultures were obtained from mature isolates. Serial dilutions were performed to achieve a concentration of <50 spores ml^{-1} (dilution 10^{-6}). This dilution (100 µl) was plated on PDA and incubated at 23–26 °C for 10 days.[37] Afterward, the strain showing a fungal colony unequivocally arising from a single conidium was selected for DNA extraction. Mycelium was extracted from PDA using a Drigalski spatula, lyophilized, ground (using a drill with a sterile pistil) and weighed. Total genomic DNA was extracted using the cetyl trimethyl ammonium bromide (CTAB) extraction protocol.[38] First, 500 µl of CTAB buffer (2% CTAB v/v, 2 M Tris–HCl pH 8, 0.5 M EDTA pH 8, 2.5 M NaCl, 1% polyvinylpyrrolidone, 0.4% v/v 2-mercaptoethanol) was added to an Eppendorf tube containing 100 mg of fungal lyophilizate and stirred gently. The mixture was placed in a 65 °C water bath for 60 min. Subsequently, 100 µl of chloroform/isoamyl alcohol (24:1) was added to the mixture, vortexed and centrifuged at 11 000 *g* (4 °C) for 5 min. The upper phase of the mixture was transferred to a new tube and a second extraction with chloroform/isoamyl alcohol (24:1) was performed. Afterward, 330 µl of isopropanol (98.5%) was added to the sample and placed at −20 °C for 2 h (to propitiate the precipitation of nucleic acids). The tube was then centrifuged for 10 min at 11 000 *g* (4 °C). The supernatant was discarded and 500 µl of 70% ethanol was added to the pellet and centrifuged at 11 000 *g* (4 °C) for 10 min. The supernatant was discarded, and the tube was air-dried under laminar flow for 30 min. The pellet was rehydrated in 50 µl of Milli-Q water and run in a 2% agarose gel to corroborate the integrity of the obtained DNA.

The internal transcribed spacer (ITS) region of the fungal DNA was amplified using primers ITS4 and ITS5[39] (Table S1). A polymerase chain reaction (PCR) was performed using a cycler (Applied Biosystems), following the protocol proposed by Zhang *et al.*[40] The reaction mixture contained KCl (50 mM), $MgCl_2$ (2.5 mM), Tris–HCl pH 8.3 (10 mM), dTTP, dATP, dGTP and dCTP (0.2 mM), primers (50 pmol), *Taq* DNA polymerase (Invitrogen) (2.5 units) and fungal DNA (25 ng) in a final volume of 50 µl. Reactions were performed by setting the thermocycler as follows: 1 cycle at 96 °C for 3 min and 30 cycles at 94 °C for 1 min, 55 °C for 1 min, and 72 °C for 2 min. The amplification efficiency was verified by 2% agarose gel electrophoresis using 5 µl of PCR products.

PCR products (30 µl) were subjected to 1.5% agarose gel electrophoresis and purified employing the Easy Pure Quick Gel Extraction Kit (TansGen Biotech). Purified DNA was then sequenced by Macrogen Inc. Sequences were edited with BioEdit software and compared with all fungal nucleotide sequences reported in the National Center Biotechnology Information (NCBI) database, employing the BLAST tool (www.ncbi.nlm.nih.gov/BLAST).

2.2 Non-thermal plasma

2.2.1 Source

A scheme of the DBD arrangement used for *in vitro* fungal treatment is shown in Figure 1. The discharge consisted of a needle matrix power electrode (total diameter 120 mm) and a flat plate-shaped ground electrode covered by a dielectric barrier of one polyester film (Thernophase 400 µm thick) and a glass Petri dish in which plastic Petri dishes containing PDA and fungal structures to be treated were placed. A high-voltage sine AC of 25 kV

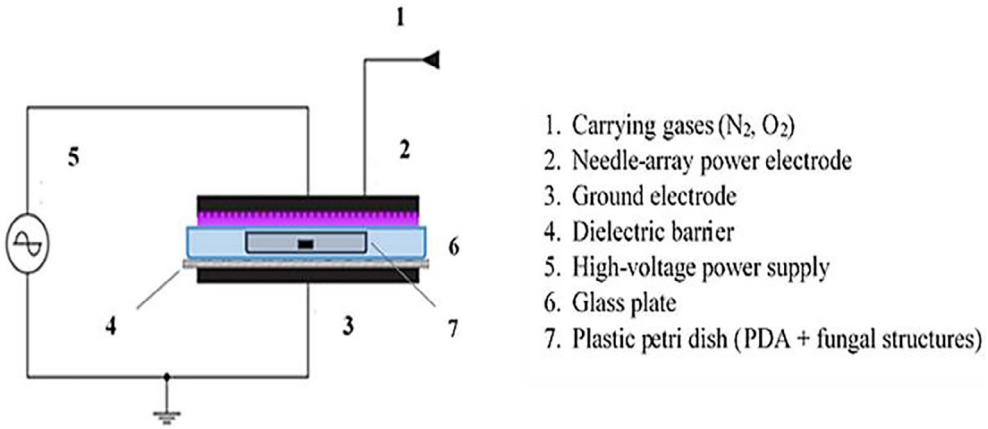

FIGURE 1. Dielectric barrier discharge arrangement used for *in vitro* fungal treatment.

was applied between the discharge electrodes at an operating frequency of 50 Hz. The prototype was adjusted to achieve a constant distance of 14 mm between the tip of the needles (of the discharge electrode) and agar surface, allowing direct contact between fungi and plasma for 3 min. In all cases, the discharge electrode completely covered the 9 cm diameter plastic Petri dish area. Because both the glass and plastic Petri dishes behaved as a dielectric barrier to the discharge, the thickness of the agar layer was carefully measured to ensure uniformity in the different treatments. However, the high water content of agar suggests that small variations in the thickness of the agar layer do not have large effects on the capacitance of the effective dielectric barrier.

For the application reported here, it is very desirable that the (long-lived) reactive plasma species generated in the plasma active region be transported towards the sample. To achieve this, oxygen or nitrogen gas (purity over 99.5%) was injected into the unconfined discharge region as carrier gases, with a gas flow rate (measured) of 6 standard liter per minute (slm). However, the gas flow did not directly affect the sample as it spread over a large area of several cm^2 in the plane in which the sample is located. The electrical parameters of the discharge were monitored by using a four-channel oscilloscope (Tektronix TDS 2004C with a sampling rate of 1 GS s^{-1} and an analogical bandwidth of 70 MHz). The discharge voltage was measured by using a high-impedance voltage probe (Tektronix P6015A, 1000×, 3pf, 100 MΩ). The power consumption in the discharge was measured by the Lissajous method,[41] inserting a 0.5-μF capacitor in series with the discharge. Charge–voltage characteristics of the discharge for the two carrier gases used in the experiments are shown in Figure 2. It is seen that the shape of the charge–voltage characteristics resembles an ellipse rather than an ideal parallelogram, as in ozonizers. Still, a total discharge capacitance of ~70 pF can be inferred in the framework of a simplified electrical model.[41] As expected, the discharge power is significantly higher (~29%) for nitrogen (22 W) than for oxygen (17 W). The difference may be related to an increase in electron losses due to an increase in the attachment processes[42] when oxygen molecules are injected into the discharge zone. The temperature of the discharge walls was measured with an infrared handheld thermometer. It never exceeded 40 °C during the experiments.

Ozone generated by the DBD arrangement was also measured in the unconfined discharge zone by UV absorption spectroscopy. An argon/mercury lamp (Avantes AvaLight–CAL–Mini,

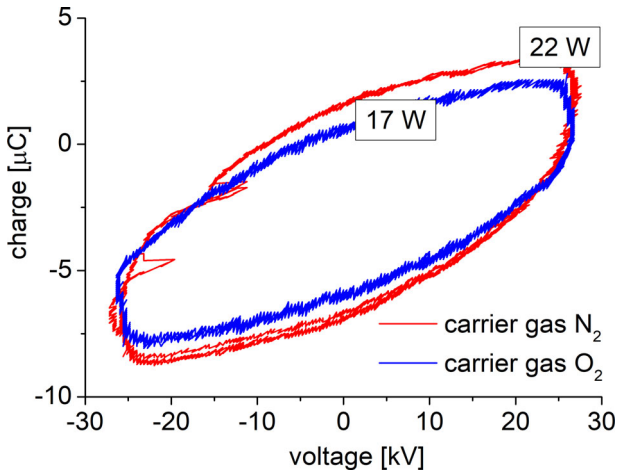

FIGURE 2. Charge–voltage characteristics of the discharge for conditions used in the treatments.

253.6–922.5 nm) was used as the UV source. The point light source was constructed by focusing the UV light through a condenser UV lens (focal length 20 mm) onto a pinhole (400 μm in diameter). The pinhole was placed in the focal plane of a UV lens (focal length 100 mm) which creates the collimated light passing through the discharge effluent. A second UV lens (focal length 100 mm) was used to project it onto the entrance slit of a UV–Vis monochromator (OBB, grating 2400 lines mm^{-1}, blazed at 300 nm). A photomultiplier (Hamamatsu R6350) attached to the monochromator converts the light signal into an electrical signal. The intensity of UV light at 254 nm was used to calculate ozone density based on Beer's law. The photoabsorption cross-section used was 1.147×10^{-21} m^2.[43] The optical path length was 130 mm (i.e., measurements represent mean values of ozone density over the diameter of the power electrode). The time resolution and detection limit of the measurements were ~0.5 s and 3 ppm, respectively.

Figure 3 shows time evolution profiles of ozone density along the whole processing time ($t = 3$ min) for the two different carrier gases used in the experiments. It is seen that in both cases, the ozone density increased for the initial seconds and reached a steady-state at ~25 s. However, for oxygen, the steady-state density value (~25–30 ppmv) was higher than that for nitrogen (15

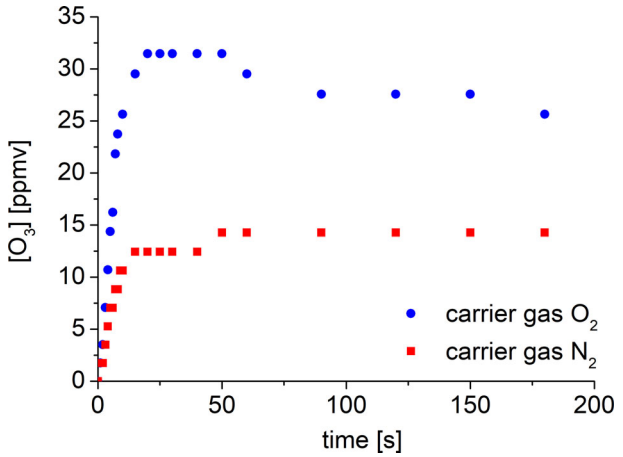

FIGURE 3. Time evolution of ozone density in the discharge effluent for conditions used in the treatments.

TABLE 1. Description of NTP treatments

Dielectric barrier	Carrying gas	Exposition time (min)	Nomenclature
Thernofase	N_2	3	TN3
	O_2	3	TO3
Control			C

ppmv) by a factor of ~2. Furthermore, it is observed that the slope of the ozone density profile at $t = 0$ also increased for oxygen, indicating that the net rate of ozone generation increased when this gas was injected into the discharge. Because the concentration of atomic oxygen (O) determines the slope of the rising rate of ozone density (through the reaction[44] $O + O_2 + M \rightarrow O_3 + M$, where M is a third body), the observed increase in ozone density may be related to an increase in the density of O atoms when the oxygen concentration in the discharge rises. Other reactive species concentrations (as NO_2) could not be experimentally determined because both the absorption cross-sections and the concentrations are relatively much lower than that of O_3. These results suggest that the air DBD was operated in the ozone mode. It should be noted that a small overestimation in the measured O_3 concentration may still be expected under the considered conditions due to superposition of absorbance from other low-concentration air species (such as NO_2 and N_2O_4) over the considered wavelength.

2.2.2 *Treatments*

To evaluate the effects of NTP on fungal growth, 5 mm diameter mycelial bites (cut from the edge of fungal isolates) were transferred to plastic Petri dishes containing PDA (25 ml) and incubated 24 h at 23–26 °C. NTP treatments were performed directly in the dishes, employing different types of carrying gases (Table 1). Before performing each treatment, the initial fungal growth halo was marked below each dish, indicating the starting point for growth measurements. Untreated isolates were employed as controls. Following plasma treatments, dishes were sealed with film, placed in an incubation chamber (23–26 °C with alternating cycles of 12 h of fluorescent light and 12 h of darkness) and subjected to daily growth measurements ($n = 9$) until control dishes were completely covered by mycelia. At the end of these measurements, subcultures were performed: bites of 5 mm diameter were obtained from the edges of isolates, transferred to new dishes with PDA medium (25 ml), maintained in an incubation chamber (under the conditions described above) and monitored to construct subculture growth curves ($n = 9$). Fifteen days after plasma exposure, the original colonies were used to determine fungal fresh weight ($n = 6$), enzymatic activities ($n = 6$) and lipid peroxidation ($n = 6$). Some dishes were maintained in the incubation chamber for 40 days, at which time they were used to determine spore number ($n = 6$) and viability ($n = 6$). The experiment had a completely randomized arrangement and was repeated twice. To evaluate conidial sensibility to NTP exposure, conidial suspensions were prepared from the original colonies (40 days old). The suspension (100 µl) was plated into Petri dishes, containing 25 ml of PDA, and exposed to plasma treatments. Percentage spore germination inhibition was recorded. The experiment was repeated twice, with five repetitions per treatment ($n = 6$).

2.3 Biometric parameters

2.3.1 *Fungal growth*

At 24-h intervals, mycelial growth diameters were measured considering the average of two crossed diameters drawn below Petri dishes and taking the center of the inoculum-bite as an intersection.[44] Measurements were prolonged until maximum growth (i.e., full dish) was visualized in the non-treated dishes (controls). The obtained values were used to construct growth curves. From these curves, the corresponding quadratic functions were obtained and then solved by calculating definite integrals (considering the values $x_1 = 0$, $x_2 = 96$ and $y = 0$), obtaining the area under the growth curve (AUC) for each treatment and repetition. The calculated AUC values were expressed in quadratic units (u^2) and used for comparative purposes.

2.3.2 *Sporulation and conidial viability*

To evaluate fungal sporulation capacity (conidiogenesis), 10 ml of saline solution (containing 9 g of NaCl and 1 ml of Tween 80 per liter of sterile distilled water) were added to each Petri dish and spores were removed with the help of a straight-headed Drigalski spatula. A 10^{-1} conidia dilution was prepared by adding 1 ml of mother conidia suspension to a tube containing 9 ml of saline solution. Then, 10 µl was taken from the conidia dilution and placed in a Neubauer chamber. The conidia concentration was determined using an optical microscope (×40). The spore count was performed three times and the average concentration was expressed as the number of spores ml^{-1}, according to Lemus.[45] Percentage of sporulation inhibition (SI%) by plasma treatment was calculated as:

$$SI\% = (\text{Number of spores}_{\text{Control}} - \text{Number of spores}_{\text{NTP}}) / \text{Number of spores}_{\text{Control}} * 100. \quad (1)$$

For conidial viability analysis, serial dilutions were prepared starting from the 10^{-1} dilution: 1 ml of this dilution was transferred to a tube containing 9 ml of saline solution, thus obtaining a 10^{-2} dilution. The same procedure was repeated until the dilution 10^{-5} was obtained. The last dilution was chosen so that the results could be adjusted to the limit of colony-forming units (CFU) detection. Aliquots of this dilution (100 µl) were plated on

dishes containing 25 ml of PDA and incubated at 23–26 °C for 3 days. The number of CFU per dish was then counted and used to calculate the percentage conidial viability inhibition (VI%) by plasma treatment[46]:

$$VI\% = 100*(1 - \text{Number of } CFU_{NTP} / \text{Number of } CFU_{Control}) \quad (2)$$

2.3.3 *Fungal fresh weight*

To obtain the fungal fresh weight all the mycelium contained in each Petri dish was removed with the help of a spatula and weighed using a precision balance (0.0001 g).

2.4 Biochemical parameters

2.4.1 *Lipid peroxidation*

Fungal mycelia were swept from dishes using a spatula. Samples were weighed and then homogenized with 20% (w/v) trichloroacetic acid, in a 1:10 (w/v) ratio. Homogenates were centrifuged at 3000 *g* for 20 min and the resulting supernatants were used for the quantification of malondialdehyde (MDA) content according to Pérez Pizá *et al.*[31] The results were expressed as nmol MDA g sample^{-1}.

2.4.2 *Antioxidant defenses*

2.4.2.1. Enzyme extraction. Fungal mycelia were swept from PDA dishes with the help of a Drigalski spatula. Samples were weighed and then ground and homogenized with 50 mM phosphate extraction buffer pH 7.4 (containing 1 mM EDTA, 1 mg polyvinylpyrrolidone and 0.5% (v/v) Triton X-100) in a 1:10 ratio. Homogenates were centrifuged at 13 000 *g* for 30 min (4 °C) and the supernatant fraction was used for enzyme assays.

2.4.2.2. Enzyme assays. Catalase activity (CAT) was measured according to Pérez Pizá *et al.*[31] and the results expressed in μmol min^{-1} mg protein^{-1}. Superoxide dismutase (SOD) activity was measured according to Becana *et al.*[47] The reaction mixture contained 2.2 μM riboflavin, 14.3 mM methionine, 82.5 μl nitro blue tetrazolium (NBT) and 5–25 μl enzyme extract in 50 mM phosphate buffer (pH 7.8) to a final volume of 250 μl. SOD activity was determined by measuring the ability of the enzyme extract to inhibit the photochemical reduction of NBT. Transparent plates (96 wells) containing the mixtures, were shaken and placed 30 cm from a light bank. The reduction of NBT was monitored by reading the absorbance at 560 nm for 10 min (a reading was taken every 2 min of exposure to light). SOD activity was expressed as U mg protein^{-1}, where 1 unit of SOD represented the enzyme activity that inhibited the photoreduction of NBT to blue formazan by 50%. Protein content in fungal extracts was determined according to Bradford.[48]

2.5 Conidia susceptibility to NTP exposure

To prepare conidial suspensions, 10 ml of saline solution (9 g of NaCl and 1 ml of Tween 80 per L of water) were placed in Petri dishes containing sporulated colonies. Spores were removed with the help of a straight-headed Drigalski spatula and formed the mother conidial suspension. A 10^{-1} conidia dilution was prepared by adding 1 ml of the mother conidia suspension to a tube containing 9 ml of saline solution. To determine the conidial concentration, 10 μl of this dilution was placed into a Neubauer chamber and the total number of conidia was calculated as described in Section 3.2. Serial dilutions were prepared from the 10^{-1} dilution: 1 ml of this dilution was transferred to a tube containing 9 ml of saline solution, giving a 10^{-2} dilution. The same procedure was repeated until a 10^{-5} dilution was obtained. The 10^{-5} dilution (100 μl) was dispersed in Petri dishes containing PDA using a spatula. This concentration was chosen so that the results could be adjusted to the CFU detection limit. After plasma treatment, colonies were kept in a culture chamber for 48 h, after which time the number of CFU per plate was determined and the conidia inactivation percentage (CI%) by plasma was calculated:

$$CI\% = 100*(1 - \text{Number } CFU_{NTP} / \text{Number } CFU_{Control}) \quad (3)$$

2.6 Statistical analysis

All data are presented as mean ± standard error (SE) of *n* replicates. Analyses were performed using the statistical software package R Commander 3.1.2 (2014). After testing for the assumption of the normal distribution and homoscedasticity, the variance ($P < 0.05$) of the obtained data was analyzed by one-way variance analysis (ANOVA). Honestly significant difference (Tukey's HSD) was obtained for all pairwise comparisons at $P < 0.05$.

3 RESULTS

3.1 Morphological and molecular characterization of fungal strain

Morphological observations of D/P fungal isolates were used for the initial classification. All isolates produced: white mycelia with occasional yellow-greenish areas (turning light brown with age) (Figure S2C); long-beak pycnidia, usually in clusters (Figure S2B); hyaline, ellipsoidal and guttulated alpha-conidia (Figure S2A); and black stroma, usually large and widespread (in some cases were circular), small in diameter (2–5 mm) (Figure S2C). None of the isolates exhibited teleomorph (Figure S2D). Regarding molecular identification, the obtained amplification products had a size of 591 bp for ITS4 and 601 bp for ITS5. The sequences of fungal DNA regions, amplified with the ITS4–ITS5 primers, are shown in Table S2. After comparing the obtained nucleotide sequences with those published in the NCBI-BLAST database, 100% of homology with *D. longicolla* (# NCBI Type) was found.

3.2 Growth and sporulation

Growth curves of D/P colonies exposed to plasma treatments (TN3 and TO3) and their subcultures, as well as the untreated controls, are shown in Figure 4. Fungal colonies exposed to plasma treatments (TN3 and TO3) exhibited growth curves below the control (Figure 4A). The AUCs showed significant differences between treated colonies and the control (Table 2), with an average inhibition effect of fungal growth of 22% for plasma treatments. The corresponding subcultures show the same behavior as the original colonies regarding inhibition of fungal growth (Figure 4B and Table 2), but the curves also show that the overall growth of subcultures corresponding to TN3- and TO3-treated colonies was reduced by an initial lag phase of treated colonies in the first 24 h.

Fungal fresh weight, 15 days after plasma application, is shown in Table 2. TN3 and TO3 colonies weighed 51% and 73% less than controls, respectively. Also, treatment TN3 registered 30% less fungal biomass than TO3. The general appearance of treated and untreated D/P colonies (40 days after plasma exposure) and the asexual reproduction structures (pycnidia) formed in each case are shown in Figure S3(A,B). Both images indicate changes in fungal colonies, regarding their appearance and ability to produce pycnidia in response to plasma exposure (TN3 and TO3).

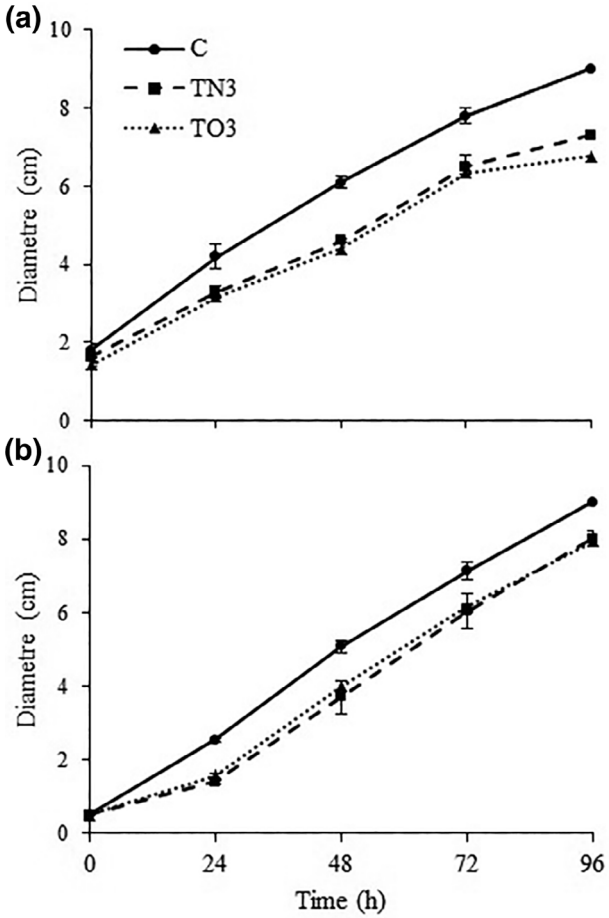

FIGURE 4. (A) Growth curves of fungal colonies exposed to NTP (TN3 and TO3) and control (C). (B) Growth curves of the correspondent subcultures. Error bars indicate standard error ($n = 9$).

Table 3 shows the average number of conidia per colony and conidial viability (denoted by the average number of CFU) as well as inhibition percentages on the number of conidia (SI%) and on conidial viability (VI%) due to plasma exposure. Plasma treatments (TN3 and TO3) inhibited between 13% and 19% the number of conidia per colony and between 50% and 80% conidial viability, compared with control colonies.

3.3 Oxidative stress and antioxidant defenses

The MDA content of fungal colonies 15 days after plasma exposition is shown in Figure 5(A). The average MDA content in treated colonies was 2.3 higher than in the control and coincided with the observed decreases in fungal growth (Figure 4A) and sporulation (Table 3). Coinciding with these results, the visual aspect of fungal colonies 15 days after plasma treatment showed considerable differences between treated colonies (TO3, TN3) and control.

Regarding antioxidant activity, both CAT (Figure 5B) and SOD (Figure 5C) activities showed differences between colonies exposed to plasma (TN3, TO3) and control colonies, although no differences were detected between the different plasma treatments. CAT activity increased four times and SOD activity was 30% higher in plasma treatments compared with the control.

3.4 Conidial susceptibility to NTP

NTP treatments applied to conidia suspensions (sown into dishes containing PDA) showed great efficacy in controlling conidial germination *in vitro* (Figure 5). Compared with control (with an average of 59 CFU per dish), both plasma treatments (TN3 and TO3) inhibited conidial germination by 99%–100%.

4 DISCUSSION

In previous studies,[31, 32] we demonstrated that NTP treatments applied to soybean seeds before sowing can effectively diminish the incidence of seed-borne D/P complex. We generated plasma

TABLE 2. Area under the growth curve (AUC) of fungal colonies exposed to NTP (TN3 and TO3) as well as their subcultures and controls, and fresh weight of the original fungal colonies 15 days after plasma application

	AUC (u^2)		
Treatment	Colonies	Subcultures	Fungal biomass (mg)
Control	569.2 ± 12.2^a	471.1 ± 16.4^a	201.8 ± 12.2^a
TN3	458.2 ± 20.3^b	371.0 ± 26.6^b	103.3 ± 3.3^c
TO3	433.9 ± 17.2^b	359.2 ± 25.6^b	146.7 ± 12.3^b

Data show mean values of replicates ± standard error (fungal growth: $n = 9$; fungal biomass: $n = 6$). Different lowercase letters indicate statistical differences between treatments and control (Dunett test, $P < 0.05$).

TABLE 3. Plasma effects on fungal sporulation, 40 days after plasma exposure (TN3 and TO3), in contrast with the control. Number of conidia per colony, conidial viability (number of colony-forming units) and inhibition percentages due to plasma exposure

Treatment	Number of conidia	Number of CFU	SI%	VI%
Control	71.0 ± 5.0^a	55.0 ± 5.0^a	—	—
TN3	62.3 ± 1.0^b	27.5 ± 2.5^b	13	50
TO3	43.5 ± 1.5^c	11.0 ± 3.0^c	39	80

Data show mean values of six replicates ± standard error ($n = 6$). Different lowercase letters indicate statistical differences between treatments and control (Dunett test, $P < 0.05$). SI%, sporulation inhibition percentage; VI%, viability inhibition percentage.

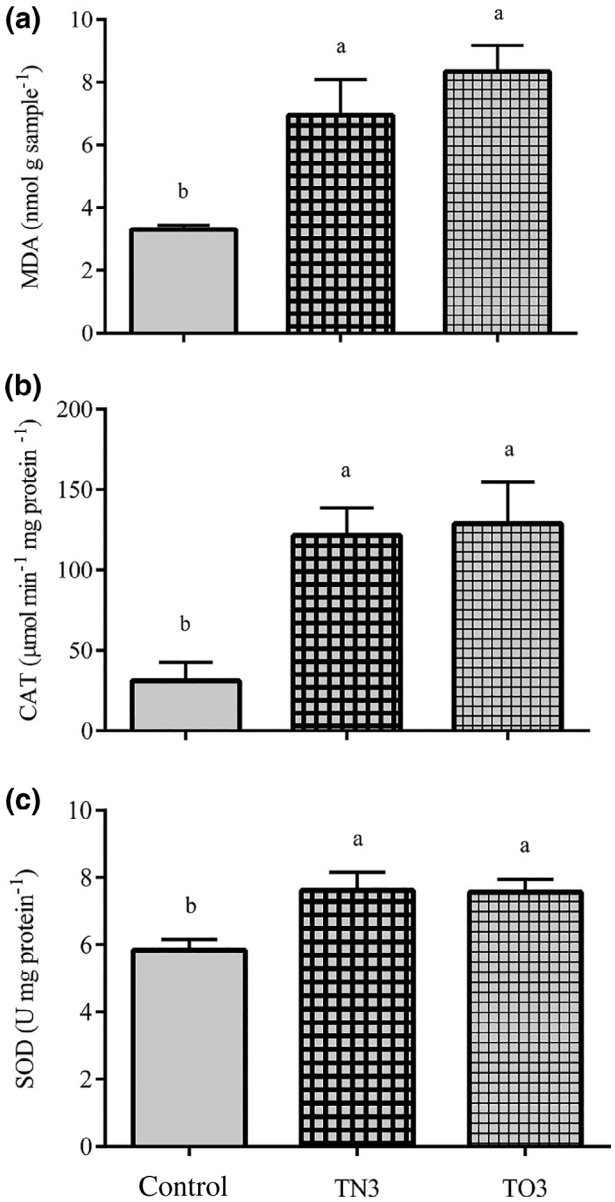

FIGURE 5. (A) Malondialdehyde (MDA) content, (B) catalase activity (CAT) and (C) superoxide dismutase activity (SOD) in D/P colonies treated with plasma (TN3 and TO3) and in control colonies, 15 days after plasma exposure. Error bars indicate standard error ($n = 6$). Different lowercase letters indicate statistical differences between treatments and control (Dunett's test, $P < 0.05$).

through DBD and demonstrated that it was able to remove D/P fungi from soybean seeds, highlighting the ability of active species to penetrate the internal tissues of seeds and eliminate fungal mycelium. The current research aimed to study the D/P fungal complex response to direct treatment with NTP and elucidate the mechanisms underlying these effects. We chose a fungal strain identified morphologically as *Diaporthe longicolla* and performed a molecular analysis to confirm its identity. This fungal strain was employed to perform our research. Considering our previous experiences working with different DBD arrangements and the inhibition of D/P growth, we chose two of the best NTP treatments for this study.

In vitro treatments of *D. longicolla* with NTP considerably reduced the growth of fungal colonies (Figure 4) with respect to untreated controls. The growth of the treated colonies shows a prolonged lag phase, which indicates that the fungus was too affected or stressed to exhibit normal growth. Therefore, the favorable growing conditions cannot be used by the fungus before growth begins.[49] However, the lag phase is not a reliable measure of stress because the length of the lag and the growth-rate inhibition are sometimes highly correlated, and sometimes not at all. Fungal growth inhibition coincided with diminished mycelial fresh weight (Table 2), which was significantly lower in both NTP treatments, TN3 and TO3, compared with control colonies. Similar results were obtained by Go *et al.*[50] and Siddique *et al.*[17] working with *Fusarium oxysporum* and *Colletotrichum* species, respectively. The oxidative power of NTP, due to the production of ROS and RNS, has been extensively demonstrated, as has the ability of plasma to destroy microbial cells through oxidative damage.[51] Because ROS can cause severe damage to DNA, protein and lipids when present at high levels, organisms have evolved defense systems (non-enzymatic molecules and enzymatic scavengers) to cope with ROS accumulation. Because the fungal cell wall and cell membrane are the first structures to come into contact with plasma components, Šimončicová *et al.*[20] related the morphological changes observed in the appearance of *Aspergillus flavus* colonies exposed to NTP to the effects of ROS on the fungal cell: erosion of the cell surface, desiccation of the cell wall, oxidation of cell wall polysaccharides and peroxidation of membrane lipids. Also, Daeschlein *et al.*[26] found that plasma can interact with water molecules present in the humid air above the agar in the dishes, leading to the formation of hydroxyl radicals, which together with other ROS, constitute the lethal components of plasma. Our data suggest that the initial oxidative burst brought about in fungal colonies upon exposure to plasma can trigger antioxidant responses to scavenge excess ROS, thereby preventing fungal cells from damage. When the ROS level within the cell is high and sustained, and the defense system cannot counteract it and oxidative stress supervenes. Interestingly, we registered oxidative damage 15 days after plasma treatment (high lipid peroxidation), accompanied by an exacerbated antioxidant activity, indicating that fungal cells were still trying to cope with the oxidative stress generated by the plasma. From our experience, hydrogen peroxide (H_2O_2) may mediate these effects because it is a stable non-radical molecule with a long enough half-life to diffuse a few micrometers within the cell. H_2O_2 is synthesized by common metabolic reactions, by leaky electron transfer, but also by particular reactions designed for the sole purpose of creating ROS. Although H_2O_2 can cause oxidative damage in cells, in this case it appears to act as a signaling molecule. Therefore, we propose that H_2O_2 may have perpetuated the detrimental effects of plasma on the exposed fungal colonies.

Regarding fungal sporulation, both NTP treatments (TN3 and TO3) significantly inhibited the ability of colonies to produce pycnidia and spores (conidia) (Figure S3) and the viability of these spores to germinate, registering significant decreases in the number of CFU per dish (Table 3). However, the TO3 treatment was superior to TN3 in these parameters. As shown in Figure 3, both treatments rapidly reached a steady-state concentration of ozone, but the O_3 density in the plateau was twice as high for TO3 than for TN3. This phenomenon might explain the differential effect on sporulation and spore viability observed between the NTP treatments, TN3 and TO3. In a recent study, Ambrico *et al.*[53] assessed the inactivation of different fungal species employing NTP and highlighted the critical role of ozone in deepening the

cell damage brought about by etching and other reactive species generated by the plasma. Taking this into account, we suggest that the higher density of ozone registered for the TO3 treatment could have enhanced cell disruption, affecting more deeply the capacity of colonies to form the reproductive structures.

Considering these findings and aiming to uncover the mechanisms underlying the effects of NTP on the biological performance of fungal colonies, we continued our research analyzing lipid peroxidation through the quantification of MDA content, as a measure of the degree of oxidative stress suffered by the colonies after exposure to plasma (Figure 5A). The MDA content of colonies exposed to NTP was greater than that of untreated controls. These results were accompanied by the determination of antioxidant enzyme activities, CAT (Figure 5B) and SOD (Figure 5C). We observed significant increases in the activity of both enzymes in colonies exposed to NTP compared with control colonies. Taken together, our observations infer that NTP treatments caused oxidative stress to hyphal cells, affecting the structure of cell membranes, causing loss of functionality and determining the observed decreases in growth (Figure 4), fresh mycelial weight (Table 2), sporulation (Figure S3) and viability of conidia (Table 3). The visual appearance of colonies exposed to NTP supported these assumptions (Figure S2). According to Panngom *et al.*,[54] cellular damage after high doses of plasma is usually accompanied by disintegration of organelles and DNA fragmentation. Also, it is well known that cell membrane lipids and proteins are primary targets of oxidation, so fungal exposition to the oxidative compounds of NTP may alter overall membrane properties and lead to cellular destruction.[53] In our work, the analysis of DNA integrity employing gel electrophoresis suggested the degradation of fungal DNA in exposed colonies (data not shown). According to Šimončicová *et al.*,[20] DNA fragmentation can occur directly by oxidation of deoxyribose or indirectly by interruption of the repair process of the oxidized bases. In this sense, we hypothesize that the production of ROS and RNS during *in vitro* fungal treatments could have triggered oxidation mechanisms that led to DNA degradation.

Filamentous fungi usually produce different types of cells and tissues: hyphae, asexual and sexual spores, conidiophores, sexual reproductive structures and chlamydospores, among others. These cells and tissues differ from each other not only in their structure and composition, but also in their biological functions.[55, 56] So it is expected that not all structures will have the same response to direct plasma treatment. In this sense, once we verified the effects of plasma on active growing mycelium, we investigated its efficacy in asexual spores (conidia) inactivation. *In vitro* treatment of conidial suspensions with NTP inhibited spore germination almost completely (Figure 6). The presence of water in the spore suspensions can increase the concentration of ROS and RNS (within them) during plasma treatments. This might have been responsible for the high efficiency of NTP in inactivating fungal spores. Moreover, the D/P spores are known to lack melanin, pigments that usually accumulate in the conidia of other fungal species, protecting them from damaging agents such as UV, ionizing and gamma irradiation, dehydration, extreme temperatures, the action of hydrolytic enzymes, antifungal drugs and free oxygen radicals.[57] The reduction in conidial germination observed in our research agrees with other authors who also studied the effects of NTP on spore viability of different phytopathogens.[21, 53, 58, 59] According to Ambrico *et al.*,[53] NTP is effective against a great variety of fungal conidia, reducing to undetectable levels their germinability when placed on the surface of artificial media, indicating that plasma treatment can act directly on fungal spores due to the combined effect of active chemical species (ROS and RNS) and UV lights. The damage caused by NTP treatments to fungal cell membranes was demonstrated before, through the quantification of MDA content in colonies. In the case of spores, NTP treatments may bring about an exacerbated oxidative stress due to the higher concentrations of ROS and RNS reached within the suspensions. Oxidative damage could have compromised spore viability, leading to an efficient inactivation. This result is in agreement with Dasan *et al.*, Yoshino *et al.*,[60] Go *et al.*[51] and Ambrico *et al.*,[53] who observed that fungal spores exposed to NTP can present aggregation, structural changes, cell wall and membrane disruption, etching, perforation, cracking and/or surface erosion.

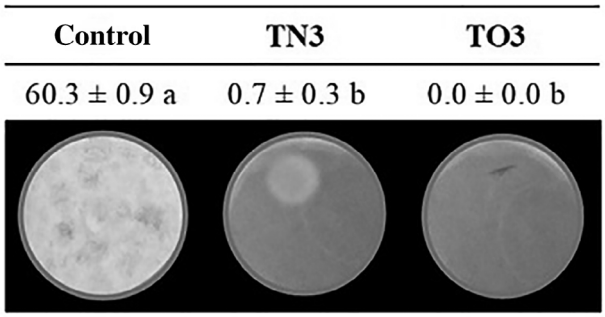

FIGURE 6. Effect of NTP treatment on the number of germinated conidia (colony-forming units) per dish, 4 days after performing NTP treatments (TN3 and TO3) to dishes containing PDA and seeded with conidial suspensions, as well as the untreated control. Data show mean values of six replicates ± standard error ($n = 6$). Different lowercase letters indicate statistical differences between treatments and control (Dunett's test, $P < 0.05$).

5 CONCLUSIONS

This research showed that direct treatment of *D. longicolla* colonies with NTP inhibits fungal growth, severely compromises the ability of colonies to produce conidia and the viability of these structures. Both evaluated plasma treatments (TN3 and TO3) led to lipid peroxidation, activation of enzyme antioxidant defenses and DNA fragmentation in the exposed colonies. Moreover, we found that NTP not only has harmful effects on mycelium, but is also useful in the inactivation of asexual spores. The use of oxygen in the generation of plasma had the same qualitative effects on fungus as nitrogen; however, quantitatively, the treatment with oxygen (TO3) exposed certain superiority over the treatment with nitrogen (TN3) in some of the evaluated parameters. The mechanisms visualized in this research helped us to explain the effectiveness of NTP in controlling the presence of D/P complex in soybean seeds, despite the clear differences between the studied systems (fungus–agar and fungus–seed). Further research is on-going to explore the potential of this technology for commercial-scale applications.

ACKNOWLEDGMENTS

This work was supported by grants from: Universidad Tecnológica Nacional (PID 5447), Agencia Nacional de Promoción Científica y Tecnológica (PICT 2015 N°1553), Universidad de Buenos Aires (UBACYT 20020160100031). KB, CZ, LP, DS-C and GY are members of CONICET. EC and MF thank CONICET for their doctoral fellowships. MCP-P, JCC and PV thank CONICET for their postdoctoral

fellowships. We are immensely grateful to Magdalena Gantuz, Verónica Noé Ibáñez, María Victoria Bertoldi, Carlos Marfil and Ricardo Masuelli (IBAM, CONICET-UNCuyo) who provided scientific support and expertise that greatly assisted this research.

SUPPORTING INFORMATION

Supporting information may be found in the online version of this article.

REFERENCES

1 Grijalba PE, del Ridao A C and Guillin E, Caracterización taxonómica y análisis de la variabilidad del agente causal del cancro del tallo de la soja en Buenos Aires (2005/2007). *Rev Investig Agropecu* **37**: 290–297 (2011).
2 Grijalba PE and del C Ridao A, Tasa de crecimiento y patogenicidad de aislamientos de aislamientos de Diaporthe phaseolorum var. caulivora. *Phyton* **83**:325–332 (2014).
3 Grijalba P, Variabilidad morfológica, genética y patogénica de *Diaporthe phaseolorum* var. *caulivora* causante del cancro del tallo de la soja en la provincia de Buenos Aires. *Tesis Magister Scientiae en Producción Vegetal*, Facultad de Ciencias Agrarias, Universidad Nacional de Mar del Plata (2011).
4 Berkland TD, Soybean seed production: Decisions and their relationship to seed quality. MSc Thesis in Agronomy, Iowa State University (2011).
5 Sánchez MC, Ridao ADC and Colavita ML. Diaporthe caulivora: agente causal de cancro del tallo predominante en cultivos de soja del sudeste bonaerense. *FAVE Sección Ciencias Agrarias*. **14**:141–160 (2015).
6 Vrandecic K, Jurkovic D and Cosic J, Effect of *Diaporthe/Phomopsis* species isolated from soybean and *Abutilon theophrasti* on soybean seed germination. *J Phytopathol* **154**:725–728 (2006).
7 Malvick DK, Pod and stem blight, stem canker and *Phomopsis* seed decay of soybeans. *Rep Plant Dis* **1997**:1–6 (1997).
8 Ploper LD and Backman PA, Nature and management of fungal diseases affecting soybean stems, pods and seeds. *Pest Manage Soybean*. Netherlands: Springer, Dordrecht, 174–184 (1992).
9 Oerke EC, Crop losses to pests. *J Agric Sci* **144**:31–43 (2006).
10 Navi SS, Huynh T, Mayers CG and Yang XB, Diversity of *Pythium* spp. associated with soybean damping-off, and management implications by using foliar fungicides as seed treatments. *Phytopathol Res* **1**:8 (2019).
11 Selcuk M, Oksuz L and Basaran P, Decontamination of grains and legumes infected with *Aspergillus* spp. and *Penicillum* spp. by cold plasma treatment. *Bioresour Technol* **99**:5104–5109 (2008).
12 Ding H, Fu TJ and Smith MA, Microbial contamination in sprouts: how effective is seed disinfection treatment? *J Food Sci* **78**:R495–R501 (2013).
13 Waskow A, Betschart J, Butscher D, Oberbossel G, Klöti D, Büttner-Mainik A *et al*., Characterization of efficiency and mechanisms of cold atmospheric pressure plasma decontamination of seeds for sprout production. *Front Microbiol* **9**:1–15 (2018).
14 Bourke P, Ziuzina D, Boehm D, Cullen PJ and Keener K, The potential of cold plasma for safe and sustainable food production. *Trends Biotechnol* **36**:615–626 (2018).
15 Misra NN, Tiwari BK, Raghavarao KSMS and Cullen PJ, Non-thermal plasma inactivation of food-borne pathogens. *Food Eng Rev* **3**: 159–170 (2011).
16 Butscher D, Van Loon H, Waskow A, von Rohr RP and Schuppler M, Plasma inactivation of microorganisms on sprout seeds in a dielectric barrier discharge. *Int J Food Microbiol* **238**:222–232 (2016).
17 Siddique SS, St. J. Hardy GE and Bayliss KL, Cold plasma as a novel treatment to reduce the *in vitro* growth and germination of *Colletotrichum* species. *Plant Pathol* **68**:1361–1368 (2019).
18 Hertwig C, Meneses N and Mathys A, Cold atmospheric pressure plasma and low energy electron beam as alternative non-thermal decontamination technologies for dry food surfaces: a review. *Trends Food Sci Technol* **77**:131–142 (2018).
19 Moreau M, Orange N and Feuilloley MGJ, Non-thermal plasma technologies: new tools for bio-decontamination. *Biotechnol Adv* **26**: 610–617 (2008).
20 Šimončicová J, Kaliňáková B, Kováčik D, Medvecká V, Lakatoš B, Kryštofová S *et al*., Cold plasma treatment triggers antioxidative defense system and induces changes in hyphal surface and subcellular structures of *Aspergillus flavus*. *Appl Microbiol Biotechnol* **102**: 6647–6658 (2018).
21 Lu Q, Liu D, Song Y, Zhou R and Niu J, Inactivation of the tomato pathogen *Cladosporium fulvum* by an atmospheric-pressure cold plasma jet. *Plasma Processes Polym* **11**:1028–1036 (2014).
22 Ochi A, Konishi H, Ando S, Sato K, Yokoyama K, Tsushima S *et al*., Management of bakanae and bacterial seedling blight diseases in nurseries by irradiating rice seeds with atmospheric plasma. *Plant Pathol*. **66**:67–76 (2017).
23 Alkawareek MY, Gorman SP, Graham WG and Gilmore BF, Potential cellular targets and antibacterial efficacy of atmospheric pressure non-thermal plasma. *Int J Antimicrob Agents* **43**:154–160 (2014).
24 Zhang X, Liu D, Zhou R, Song Y, Sun Y, Zhang Q *et al*., Atmospheric cold plasma jet for plant disease treatment. *Appl Phys Lett* **104**: 043702 (2014).
25 Stoffels E, Kieft IE, Sladek REJ, Van den Bedem LJM, Van der Laan EP and Steinbuch M, Plasma needle for *in vivo* medical treatment: recent developments and perspectives. *Plasma Sources Sci Technol* **15**: S169–S180 (2006).
26 Daeschlein G, Scholz S, von Woedtke T, Niggemeier M, Kindel E, Brandenburg R *et al*., *In vitro* killing of clinical fungal strains by low-temperature atmospheric-pressure plasma jet. *IEEE Trans Plasma Sci* **39**:815–821 (2011).
27 Basaran P, Basaran-Akgul N and Oksuz L, Elimination of *Aspergillus parasiticus* from nut surface with low pressure cold plasma (LPCP) treatment. *Food Microbiol* **25**:626–632 (2008).
28 Won MY, Lee SJ and Min SC, Mandarin preservation by microwave-powered cold plasma treatment. *Innov Food Sci Emerg Technol* **39**: 25–32 (2017).
29 Zahoranová A, Hoppanová L, Šimončicová J, Tučeková Z, Medvecká V, Hudecová D *et al*., Effect of cold atmospheric pressure plasma on maize seeds: enhancement of seedlings growth and surface microorganisms inactivation. *Plasma Chem Plasma Process* **38**:969–988 (2018).
30 Misra NN, Yadav B, Roopesh MS and Jo C, Cold plasma for effective fungal and mycotoxin control in foods: mechanisms, inactivation effects, and applications. *Compr Rev Food Sci Food Saf* **18**:106–120 (2019).
31 Pérez-Pizá MC, Prevosto L, Zilli C, Cejas E, Kelly H and Balestrasse K, Effects of non-thermal plasmas on seed-borne *Diaporthe/Phomopsis* complex and germination parameters of soybean seeds. *Innov Food Sci Emerg Technol* **49**:82–91 (2018).
32 Pérez-Pizá MC, Prevosto L, Grijalba PE, Zilli CG, Cejas E, Mancinelli B *et al*., Improvement of growth and yield of soybean plants through the application of non-thermal plasmas to seeds with different health status. *Heliyon* **5**:1–33 (2019).
33 ISTA, Validated Seed Health Testing Methods, in 2017 International Seed Testing Association Chapter 7, 7-016 (2017).
34 Scandiani MM and Luque AG, Identificación de patógenos en semilla de soja. *Análisis Semillas Supl Espec* **2**:148 (2009).
35 Pioli RN, Morandi EN, Martínez MC, Lucca F, Tozzini A, Bisaro V *et al*., Morphologic, molecular, and pathogenic characterization of *Diaporthe phaseolorum* variability in the core soybean-producing area of Argentina. *Phytopathology* **93**:136–146 (2003).
36 Hernández FE, Pioli RN, Peruzzo AM, Formento ÁN and Pratta GR, Caracterización morfológica y molecular de una colección de aislamientos de *Phomopsis longicolla* (Teleomorfo desconocido: *Diaporthales*) de la región templada y subtropical de Argentina. *Rev Biol Trop* **63**: 871–884 (2015).
37 Cañedo V and Ames T, Medios de cultivo de Laboratorio, in *Manual de Laboratorio para el manejo de Hongos Entomopatógenos*. International Potato Center, Peru, pp. 18, 18–22, 22 (2004).
38 Rogers SO and Bendich AJ, Extraction of DNA from milligram amounts of fresh, herbarium and mummified plant tissues. *Plant Mol Biol* **5**: 69–76 (1985).
39 White TJ, Bruns T, Lee SJWT and Taylor J, Amplification and direct sequencing of fungal ribosomal RNA genes for phylogenetics. *PCR Protoc*. **18**:315–322 (1990).

40 Zhang AW, Riccioni L, Pedersen WL, Kollipara KP and Hartman GL, Molecular identification and phylogenetic grouping of *Diaporthe phaseolorum* and *Phomopsis longicolla* isolates from soybean. *Phytopathology* **88**:1306–1314 (1998).

41 Pipa AV, Koskulics J, Brandenburg R and Hoder T, The simplest equivalent circuit of a pulsed dielectric barrier discharge and the determination of the gas gap charge transfer. *Rev Sci Instrum* **83**:115112 (2012).

42 Kossyi IA, Kostinsky AY, Matveyev AA and Silakov VP, Kinetic scheme of the non-equilibrium discharge in nitrogen–oxygen mixtures. *Plasma Sources Sci Technol* **1**:207–220 (1992).

43 Daumont D, Brion J, Charbonnier J and Malicet J, Ozone UV spectroscopy I: absorption cross-sections at room temperature. *J Atmos Chem* **15**:145–155 (1992).

44 Martínez DA, Buglione MB, Filippi MV, Reynoso LDC, Rodríguez GE and Agüero MS, Mycelial growth evaluation of *Pleurotus ostreatus* and *Agrocybe aegerita* on pear pomaces. *An Biol* **37**:1–10 (2015).

45 Lemus Y, Rodríguez G, Cuervo R, Vanegas JAD and Zuluaga CL. Determinación de la factibilidad del hongo Metarhizium anisopliae para ser usado como control biológico de la hormiga arriera (Atta cephalotes). *Revista Guillermo de Ockham*. **6**:91–98 (2008).

46 Sun P, Sun Y, Wu H, Zhu W, Lopez JL, Liu W *et al.*, Atmospheric pressure cold plasma as an antifungal therapy. *Appl Phys Lett* **98**:021501 (2011).

47 Becana M, Aparicio-Tejo P, Irigoyen JJ and Sanchez-Diaz M, Some enzymes of hydrogen peroxide metabolism in leaves and root nodules of *Medicago sativa*. *Plant Physiol* **82**:1169–1171 (1986).

48 Bradford MM, A rapid and sensitive method for the quantitation of microgram quantities of protein utilizing the principle of protein–dye binding. *Anal Biochem* **72**:248–254 (1976).

49 Chi MH, Park SY and Lee YH, A quick and safe method for fungal DNA extraction. *Plant Pathol J* **25**:108–111 (2009).

50 Meletiadis J, Meis JF, Mouton JW and Verweij PE, Analysis of growth characteristics of filamentous fungi in different nutrient media. *J Clin Microbiol* **39**:478–484 (2001).

51 Go SM, Park MR, Kim HS, Choi WS and Jeong RD, Antifungal effect of non-thermal atmospheric plasma and its application for control of postharvest *Fusarium oxysporum* decay of paprika. *Food Control* **98**:245–252 (2019).

52 Martindale JL and Holbrook NJ, Cellular response to oxidative stress: signalling for suicide and survival. *J Cell Physiol* **192**:1–15 (2002).

53 Ambrico PF, Šimek M, Rotolo C, Morano M, Minafra A, Ambrico M *et al.*, Surface dielectric barrier discharge plasma: a suitable measure against fungal plant pathogens. *Sci Rep* **10**:1–17 (2020).

54 Panngom K, Lee SH, Park DH, Sim GB, Kim YH, Uhm HS *et al.*, Non-thermal plasma treatment diminishes fungal viability and up-regulates resistance genes in a plant host. *PLoS One* **9**:e99300 (2014).

55 Ouf SA, Basher AH and Mohamed AAH, Inhibitory effect of double atmospheric pressure argon cold plasma on spores and mycotoxin production of *Aspergillus niger* contaminating date palm fruits. *J Sci Food Agric* **95**:3204–3210 (2015).

56 Bistis GN, Perkins DD and Read ND, Different cell types in *Neurospora crassa*. *Fungal Genet Rep* **50**:17–19 (2003).

57 Belozerskaya TA, Gessler NN and Aver'yanov AA, Melanin pigments of fungi, in *Fungal Metabolites Reference Series in Phytochemistry*. Springer, Cham (2017).

58 Iseki S, Ohta T, Aomatsu A, Ito M, Kano H, Higashijima Y *et al.*, Rapid inactivation of *Penicillium digitatum* spores using high-density non-equilibrium atmospheric pressure plasma. *Appl Phys Lett* **96**: 153704 (2010).

59 Konishi H, Takashima K, Kato T, Kaneko T, Inawashiro S & Seo N, Sterilization effects of reactive species in atmospheric air plasma on plant pathogenic fungi, in Proceedings of Plasma Conference, Nigata, Japan. 19aD1-3 (2014).

60 Yoshino K, Matsumoto H, Iwasaki T, Kinoshita S, Noda K and Iwamori S, Monitoring of sterilization in an oxygen plasma apparatus, employing a quartz crystal microbalance (QCM) method. *Vacuum* **93**:84–89 (2013).